IEEE Access
Multidisciplinary ⋮ Rapid Review ⋮ Open Access Journal

Received April 15, 2019, accepted May 13, 2019, date of publication May 29, 2019, date of current version June 18, 2019.

Digital Object Identifier 10.1109/ACCESS.2019.2919701

Robust Altitude Stabilization of VTOL-UAV for Payloads Delivery

RAMDANE HEDJAR, (Senior Member, IEEE), AND MANSOUR ABDULAZIZ AL ZUAIR
Department of Computer Engineering, College of Computer and Information Sciences (CCIS), King Saud University, Riyadh 11543, Saudi Arabia

Corresponding author: Ramdane Hedjar (hedjar@ksu.edu.sa)

This work was supported by the Research Center of the College of Computer and Information Sciences, King Saud University.

ABSTRACT In this paper, we investigate the problem of robust altitude stabilization for the vertical take-off and landing (VTOL) of an unmanned aerial vehicle in the presence of external disturbances (e.g. wind gusts), payload variations, and noisy measurements. The design of the controller is simple; it is based on the minimization of the one-step-ahead predicted position errors. The stability analysis of the closed loop in the presence of external disturbances is presented. The analysis results prove that the tracking errors of attitude, take-off, hovering, and landing are uniformly bounded. Since the proposed control algorithm will be employed for goods delivery by drones, the robustness of this algorithm against low-frequency disturbances and payload variations is a major objective. To this end, integral action is included in the altitude loop to eliminate the induced steady-state error and to drop off the payload in the desired position successfully. Furthermore, the controller is given in the closed form to facilitate its implementation onboard to increase the autonomy of the flight. The numerical simulations are provided to show the effectiveness of the proposed algorithm.

INDEX TERMS Altitude stabilization, payload variations, predictive control, robustness, VTOL-UAV.

I. INTRODUCTION

Since unmanned aerial vehicles (UAVs) are being rapidly employed in several applications, the development of small-scale and low-cost airplanes is attracting many researchers across the world. Research on the vertical take-off and landing (VTOL) of UAV is gaining more popularity owing to its use in different civil applications including surveillance, search and rescue, and inspections of structures. A special class of this aircraft with four rotors, a quadrotor helicopter, is designed by different laboratories across the world. These quadrotor helicopters can be controlled autonomously or remotely from the ground control station. From the control point of view, they represent a highly coupled and nonlinear multivariable system with an unstable and underactuated nature, and they are subject to different aerodynamic effects such as wind gusts, sensor noises, perturbations, time delay, and payload variations.

Various methods for attitude stabilization or trajectory tracking have been presented, starting from linear model-based controllers to nonlinear model-based controllers. The well-known PID flight controllers were tested and implemented in [1]. However, the control parameters are tuned empirically by trial and error; further, the stability of the closed-loop system with disturbances and uncertainties is not provided. Many other studies implemented linear model-based controllers (LQG, MPC, H∝) that ensure closed-loop stability; it is well-known that performances will degrade when the aircraft leaves the nominal conditions. To overcome this disadvantage, many nonlinear model-based controllers have been developed and tested; for example feedback linearization control [2], [33], internal-model-control [3], [34], backstepping approach [4], [5], [6], sliding mode control [7] and differential flatness [8].

UAVs need a robust control system to resist external forces, unmodeled dynamics, and atmospheric disturbances. During the last decade, to counteract these external disturbances and unknown forces, some studies included adaptive mechanisms in the design of the controller [9], [10], [11]; observers were also been used to estimate the unmodeled dynamics and external disturbances [12]. Omari *et al.* [13] presented a dynamic model that includes both blade flapping and induced drag forces. Based on this model, they designed a hierarchical nonlinear controller to compensate for the nonlinear

The associate editor coordinating the review of this manuscript and approving it for publication was Xudong Zhao.

effects of these drag forces. Lee [14] developed an adaptive tracking controller for the attitude control of the aircraft where the inertia matrix is unknown. The authors in [15] proposed a sliding mode observer for external disturbances. There exists other new techniques that are based on adaptive neural networks [44] and fuzzy logic [45], [46], which can solve the robustness problem of the quadrotor during the flight. For instance, neural networks have been used to learn the dynamics of UAV including uncertainties such as aerodynamic frictions and blade flapping [16]. In [40], the authors combined the adaptive radial basis function neural networks (RBFNNs) and double-loop integral sliding mode method to control a quadrotor subject to disturbances, and uncertainties of parameters. In fact, the adaptive mechanism is included in the control loop to compensate for the disturbances and uncertainties. Further, in [41] the authors developed a control scheme based on wavelet NN-PID for load transportation by a quadrotor with the unknown characteristics of the suspended load. In this work, wavelet neural networks are used to adjust controller gains. The authors in [42] combined Type-2 fuzzy logic controller with neural networks for solving the trajectory tracking problem in the presence of disturbances and wind gust conditions. However, for fully autonomous navigation of these platforms, such algorithms, with high computational cost, are not suitable for onboard implementation. In fact, all algorithms for control, sensing and navigation should be performed in real-time onboard and the processors used have limited computational resources. Further, as more complex scenarios are envisaged, many researchers are working to reach the full autonomy of UAVs [30] with simple and efficient algorithms used onboard to avoid communication problems with the base station [31].

The major advantage of nonlinear model predictive control (NMPC) resides in its ability to explicitly handle input and state constraints in the controller design. The authors in [17] formulated the NMPC algorithm for planning paths under input and state constraints. Successful tracking performances of the generated position and heading trajectories are obtained. However, in nonlinear model predictive control, a nonlinear optimization problem must be solved online with computational complexity and this drawback weakens the full autonomous navigation of the aircraft. For this reason, the authors in [18] have applied NMPC to aircraft control using a field-programmable gate array (FPGA) to counteract the computational burden of the algorithm. On another hand, to avoid the computational complexity of NMPC, several nonlinear predictive laws have been developed in the past [19]–[21]. These methods are based on the approximation of the one-step-ahead predictive tracking error that is obtained by expanding the output signal and the target in a r_i^{th} order Taylor series, where r_i is the relative degree of the i^{th} output. Afterward, the deduced quadratic programming (QP) problem is used to derive the optimal control law. In addition, standard numerical procedures exist that can solve this QP fast (see for instance [43]). The work developed in this paper is the extension of the idea presented in [36]. The one-step-ahead predictive controller, used in a cascade structure, is applied to a more realistic mathematical model of UAV for the altitude stabilization of VTOL. Further, in this work, a stability analysis of the closed system in a mismatched case using the Lyapunov method is provided.

Recent years have witnessed an emergence of new civil applications of UAVs linked to aerial manipulation and transportations [26]. Therefore, many authors have studied the problem of modeling and controlling quadrotor flying with a suspended load [22]–[24]. The authors in [25] are expecting high congestion of UAVs in the airspace due to their increased use, and therefore, they proposed a layered network architecture for coordinating the access of UAVs to airspace to reduce the congestion. In fact, DHL and Amazon are some companies that are using UAVs to deliver items urgently to remote inaccessible locations [27]; this study fits the context of these applications. In addition to uncertainties and unknown disturbances, the flight is subject to payload variations that induce steady-state errors in the tracking performances. It is a challenging task to achieve this kind of mission successfully.

The main advantages of the proposed control algorithm can be summarized as follows:

- The robustness of the control algorithm in the presence of unknown and variable payloads.
- The robustness of the controller with respect to noise measurements and wind gusts.
- The stability of the tracking error is provided.
- Constraints are explicitly included in the design of the controller.
- In the unconstrained case, the control loop is given in the closed form (no online optimization). On the other hand, in the constrained case, the optimization problem is formulated as a quadratic programming problem.

Hence, the contribution of this paper relies on the integration of all these advantages in one algorithm.

Some nonlinear control methods, cited previously, may include the integral action in the loop to eliminate the steady-state error; however, these methods cannot consider constraints on control signals and/or states in the control design. Hence, most of these approaches use the saturation technique to constrain the control signal, which produces a non-optimal solution (see [29] chap.23). On another hand, in the proposed approach, constraints on control signals are included explicitly in the control design. The control algorithm is formulated as a convex optimization problem and the optimal solution can be obtained by using available fast numerical procedures (for instance quadratic programming solvers).

The application intended in this work focuses on the delivery process of payload to inaccessible positions using a small flying machine. For instance, to a mountain summit (or a terrace of a building) where people may be waiting for rescue or help. Consequently, the payload is variable and induces a steady-state error. However, to perform this task correctly,

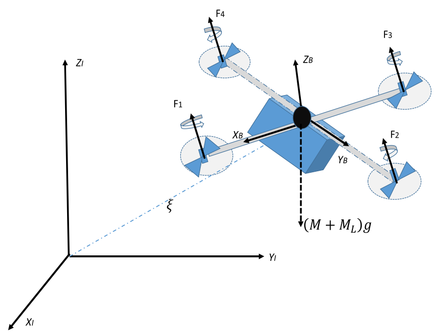

FIGURE 1. Quadrotor helicopter coordinate systems.

TABLE 1. Parameters of the UAV.

M	The total mass of the aircraft.
g	The gravitational constant (9.81 ms $^{-2}$).
F	Thrust force developed by rotors.
e_3	The unit vector $\lvert 0 \quad 0 \quad 1 \rvert^T$.
$L(t)$	The unknown variable payload ($L(t) = M_L g$).
F_{ext}	Unknown aerodynamic forces and disturbances expressed in $\{I_B\}$.
I	The inertia matrix of the aircraft.
Γ	Vector of the applied torques.
Γ_{gyro}	Gyroscope torques.

the altitude steady-state error is not tolerated to ensure the parcel is delivered to the right location. Therefore, the proposed algorithm is an effective solution for this type of applications.

The remainder of this paper is arranged as follows. In section 2, a dynamic mathematical model of the quadcopter is presented. Section 3 provides an overview of the predictive controller with its stability issue. The application of the predictive controller in the cascade structure to the UAV is described in this section. To show the effectiveness of the proposed algorithm, simulations are carried out in section 4, using the mismatched model. Further, in this section, constraints on control signals are included in the control design. Finally, section 5 provides some concluding remarks.

II. DYNAMIC MODEL OF THE UAV

The mathematical model of the UAV is widely described in different research works [1, 6, 28]. The dynamic model, with six degrees of freedom, can be split into two sub-systems: the translational movement that describes the position and the velocity of flight, and the rotational movement that describes the attitude, angular rates and moments. The mathematical model is deduced from the fundamental theorem of mechanics in two different frames: The inertial frame I_i and the body frame I_B (Fig.1).

Let $\xi = \lvert x \; y \; z \rvert^T \in \Re^3$ be the vector that describes the position of the aircraft in the inertial frame and $\eta = \lvert \phi \; \theta \; \psi \rvert^T \in \Re^3$ be a vector that describes the attitude of the vehicle in the body frame. The three Euler's angles are: ϕ, the pitch angle $\left(-\frac{\pi}{2} < \phi < \frac{\pi}{2}\right)$, θ, the roll angle $\left(-\frac{\pi}{2} < \theta < \frac{\pi}{2}\right)$; and ψ the yaw angle $(-\pi \leq \psi \leq \pi)$. Therefore, the dynamic model has the translational velocity vector given by $V = \lvert V_x \; V_y \; V_z \rvert^T$ and the rotational velocity vector represented by $\Omega = \lvert \Omega_1 \; \Omega_2 \; \Omega_3 \rvert^T$.

In order to reduce the complexity of the dynamic model, the following assumptions are adopted throughout the study:

1. The structure of the aircraft is rigid, symmetric, and the origin of the fixed aircraft-frame coincides with the center of gravity (CoG) of the aircraft.
2. Full state information is available.
3. The payload is assumed to be symmetric and homogeneous; it is attached to the body frame of the quadrotor at the position $\rho = \lvert 0 \; 0 \; -\varepsilon \rvert^T$ which is located on the Z_B-axis.
4. The thrust and drag forces are proportional to the square of the propellers speed.
5. All unstructured modeling uncertainties and noise disturbances are unknown but bounded by some known functions.

Under these assumptions, we can apply Newton's laws on the flight system when it is subject to:

- Forces and moments, acting on the CoG of the body.
- Aerodynamic effects acting mainly on the transported payload.

Hence, one can get the two sub-dynamic models as follows:

$$\Sigma_1 : \begin{cases} \dot{\xi} = R_t V \\ M\dot{V} + \Omega \times (MV) = Fe_3 + F_{ext} - (M + M_L)\, g R_t^T e_3 \end{cases} \tag{1a}$$

$$\Sigma_2 : \begin{cases} \dot{R}_t = R_t S(\Omega), \\ I\dot{\Omega} + \Omega \times (I\Omega) = \Gamma - \epsilon e_3 \times F_{ext} - \Gamma_{gyro}, \end{cases} \tag{1b}$$

where $R_t = R_\phi R_\theta R_\psi \in SO(3)$ (the 3D rotation group) is the transformation matrix between the inertial frame I_i and the body frame I_B; $S(\Omega)$ is the skew-symmetric matrix. It is known that it is difficult to locate the application point of F_{ext}. Thus, we assume that aerodynamic forces, due to wind gusts, are applied on the transported payload at point $\rho_F = \lvert 0 \; 0 \; -\epsilon \rvert^T$ located on the Z-axis of the body frame with $\epsilon > \varepsilon$.

The angular velocity $\Omega \in \Re^3$ and the linear velocity $V \in \Re^3$ are expressed in the body frame I_B. Thus, the translational dynamic of the aircraft in the inertial frame becomes

$$M\ddot{\xi} = FR_t e_3 - (Mg + L(t))e_3 + F_{ext}. \tag{2}$$

The description of UAV's parameters are listed in the following table.

The nonlinear model (1) is an underactuated system with four inputs signals, which are: the thrust force F and the control vector torque Γ, defined as

$$F = \alpha \sum_{i=1}^{4} \omega_i^2; \quad \Gamma = \begin{bmatrix} l\alpha \left(\omega_4^2 - \omega_2^2\right) \\ l\alpha \left(\omega_3^2 - \omega_1^2\right) \\ \beta \sum_{i=1}^{4} (-1)^{i+1} \omega_i^2 \end{bmatrix}, \tag{3}$$

where $\alpha > 0$ is the thrust factor, l is the distance between the CoG of the quadrotor and rotor axes, $\beta > 0$ is the drag coefficient, and $\omega_i (i = 1,4)$ is the rotational speed of the i^{th} rotor.

In this work, the dynamic model is split into two sub-subsystems: the first subsystem is represented by the altitude and attitude vector $Z_1 = (z, \phi, \theta, \psi)^T$, while the second subsystem is represented by the horizontal motion vector $Z_3 = (x, y)^T$. Since the model will be used to design the controller, external forces, disturbances, and load variations are ignored. Consequently, the nominal dynamic model of the flight is

$$\Pi_1 : \begin{cases} \dot{z}_1 = Z_2 \\ \dot{z}_2 = f(Z_1, Z_2) + G(Z_1) U(t), \end{cases} \tag{4a}$$

$$\Pi_2 : \begin{cases} \dot{Z}_3 = Z_4 \\ \dot{Z}_4 = \dfrac{F}{M} \Upsilon(\psi) V_i(t), \end{cases} \tag{4b}$$

where $\left| Z_1 \ Z_2 \right|^T \in \mathcal{R}^8$ and $U(t) \in \mathcal{R}^4$ are the state vector and the control vector of the first sub-system. The control vector can be written as a function of the angular velocities of the four rotors as

$$U(t) = \begin{bmatrix} U_1 \\ U_2 \\ U_3 \\ U_4 \end{bmatrix} = \begin{bmatrix} \alpha & \alpha & \alpha & \alpha \\ 0 & -\alpha & 0 & \alpha \\ \alpha & 0 & -\alpha & 0 \\ -\beta & \beta & -\beta & \beta \end{bmatrix} \begin{bmatrix} \omega_1^2 \\ \omega_2^2 \\ \omega_3^2 \\ \omega_4^2 \end{bmatrix}'$$

$\left| Z_3 \ Z_4 \right|^T \in \mathcal{R}^4$ and $V_i(t) \in \mathcal{R}^2$ are the state vector and the control vector of the second sub-system respectively. The other variables are defined as follows (see [1])

$$f(Z_1, Z_2) = \begin{bmatrix} \alpha_1 \dot{\psi}\dot{\theta} - a_1 \Omega_r \dot{\theta} \\ \alpha_2 \dot{\psi}\dot{\phi} + a_2 \Omega_r \dot{\phi} \\ \alpha_3 \dot{\phi}\dot{\theta} \end{bmatrix};$$

$G(Z_1) = diag\left(\cos(\phi)\cos(\theta)/M, \beta_1, \beta_2, \beta_3\right)$, $\Upsilon(\psi) = \begin{vmatrix} \cos(\psi) & \sin(\psi) \\ \sin(\psi) & -\cos(\psi) \end{vmatrix}$; $V_i(t) = \begin{vmatrix} \sin(\theta) \\ \sin(\phi) \end{vmatrix}$, J_r is the propeller inertia, $\Omega_r = \omega_1 - \omega_2 + \omega_3 - \omega_4$, $\alpha_1 = \frac{(J_{yy} - J_{zz})}{J_{xx}}$; $\alpha_2 = \frac{(J_{zz} - J_{xx})}{J_{yy}}$; $a_1 = \frac{J_r}{I_{xx}}$; $a_2 = \frac{J_r}{I_{yy}} \alpha_3 = \frac{(J_{xx} - J_{yy})}{J_{zz}}$; $\beta_1 = \frac{l}{J_{xx}}$; $\beta_2 = \frac{l}{J_{yy}}$; $\beta_3 = \frac{1}{J_{zz}}$.

III. CONTROL LAWS FOR VTOL-UAV

In this work, we are interested in controlling the position $\xi(t)$ of the aircraft in the inertial frame and the attitude in the body frame. To do so, the VTOL control structure of the aerial vehicle is considered in a two-stage process. First, the attitude and altitude controller of the aircraft are designed without considering the load variations and uncertainties. Then, the controller of the horizontal movement is considered.

A. ONE-STEP-AHEAD PREDICTIVE CONTROL

Consider the first sub-system described by (4a)

$$\Pi_1 : \begin{cases} \dot{Z}_1 = Z_2 \\ \dot{Z}_2 = f(Z_1, Z_2) + G(Z_1) U(t) \\ y(t) = Z_1(t), \end{cases} \tag{5}$$

Assumption: Both pitch and roll angles are constrained between $-\frac{\pi}{2}$ and $\frac{\pi}{2}$; thus, the matrix $G(Z_1)$ is symmetric and nonsingular $(M(Z_1) = G(Z_1)^{-1})$.

Let y_{ref} be a desired position and $e(t+h) = \left(y(t+h) - y_{ref}\right)$ be the predicted dynamic position error. The problem in one-step-ahead predictive control consists in elaborating a control law $U(Z_1, Z_2, t)$ that improves the tracking accuracy at the next step $(t+h)$. Therefore, the goal of the one-step-ahead control method is to minimize the following cost function [20]

$$J(t, y, U) = \frac{1}{2}\|e(t+h)\|_Q^2 + \frac{1}{2}\|U(t)\|_R^2, \tag{6}$$

where $Q \in \mathcal{R}^{4\times4}$ and $R \in \mathcal{R}^{4\times4}$ are positive definite and positive semi-definite matrices respectively.

A simple and effective way to predict the influence of $U(t)$ on the predicted dynamic error $e(t+h)$ is to expand it into a first order Taylor series expansion, in such a way to obtain the predicted tracking error vector

$$e(t+h) = e(t) + h\dot{e}(t) + \frac{h^2}{2} f(Z_1, Z_2) + \frac{h^2}{2} G(Z_1) U(t). \tag{7}$$

The minimization of J with respect to $U(t)$ by setting $\frac{\partial J}{\partial U} = 0$ yields the optimal predictive control law

$$U(t) = -\frac{h^2}{2}\left(\frac{h^4}{4} G(Z_1)^T Q G(Z_1) + R\right)^{-1} \times G(Z_1)^T Q \left(e(t) + h\dot{e}(t) + \frac{h^2}{2} f(Z_1, Z_2)\right). \tag{8}$$

B. STABILITY ANALYSIS IN THE MISMATCHED CASE

In order to analyze the stability of the closed-loop system in the mismatched case, the wind disturbances, load variations, and noise measurements are added to the mathematical model (5). Hence, we obtain the following model

$$\Pi_1 : \begin{cases} \dot{Z}_1 = Z_2 \\ \dot{Z}_2 = f(Z_1, Z_2) + G(Z_1) U(t) + \gamma(t) \\ y(t) = Z_1(t) + \delta(t) \end{cases} \tag{9}$$

where the vector $\gamma(\mathrm{t}) = \left| L(t) + e_3^T F_{ext} \ -\epsilon S(e_3) R_t F_{ext} \right| = \left[L(t) + \gamma_1(\mathrm{t}) \ \gamma_2(\mathrm{t}) \ \gamma_3(\mathrm{t}) \ \gamma_4(\mathrm{t}) \right]^T \in \mathcal{R}^4$ stands for the process uncertainties due to unknown load variations, disturbances, and wind gusts satisfying $\gamma(\mathrm{t}) \le \gamma_{max}$. In practice, the measured data is also noisy for several reasons: imperfect sensors and wind gusts on the craft. Therefore, $\delta(t) \in \Re^4$ denotes the added noise to the measured signals satisfying: $\delta(t) \in C^1$ and $\delta(t) \le \delta_{max}$.

The applied control vector (8), with $R = 0$, yields

$$U(t) = -\frac{2}{h^2} G(Z_1)^{-1} \left(e(t) + h\dot{e}(t) + \frac{h^2}{2} f(Z_1, Z_2) \right). \quad (10)$$

Note that the size of the control parameter h affects the rate of the convergence or time response and reduces the steady state error. To obtain the dynamic equation of the position error, we perform the following change of variables

$$e_1(t) = \mathrm{e}\,(\mathrm{t}) = Z_1(t) - Z_{1ref} \text{ and } e_2(t) = \dot{e}_1(t) \quad (11)$$

where $Z_{1ref} = \left(z_{ref}, \phi_{ref}, \theta_{ref}, \psi_{ref}\right)^T \in \mathcal{R}^4$.

Substituting equation (10) into equation (9), with the new variables given in (11), yields the following tracking error dynamics

$$\begin{cases} \dot{e}_1 = e_2 \\ \dot{e}_2 = -\dfrac{2}{h^2} e_1 - \dfrac{2}{h} e_2 - \dfrac{2}{h^2} \gamma(\mathrm{t})), \end{cases} \quad (12)$$

or under the following compact form

$$\dot{E} = \Lambda(h) E + B_h \gamma(t), \quad (13)$$

where $E = \begin{vmatrix} e_1 \\ e_2 \end{vmatrix}$, $\Lambda(h) = \begin{vmatrix} 0 & I_4 \\ -\frac{2}{h^2} I_4 & -\frac{2}{h} I_4 \end{vmatrix}$, $B_h = \begin{vmatrix} 0 \\ -\frac{2}{h^2} I_4 \end{vmatrix}$, and I_4 is the (4×4) identity matrix.

Consider a Lyapunov function candidate $V = E^T S E$ where $S > 0$ is a real symmetric positive-definite matrix. The time-derivative of V is

$$\dot{V} = E^T \left(\Lambda^T(h) S + S \Lambda(h) \right) E + 2 E^T S B_h \gamma(t). \quad (14)$$

We can show that $\Lambda(h)$ is a Hurwitz matrix (stable matrix) for any $h > 0$; therefore, there exists a symmetric positive definite matrix T solution of the Lyapunov matrix equation

$$\Lambda^T(h) S + S \Lambda(h) = -T.$$

The derivative of V is bounded by

$$\dot{V}(E) \le -\lambda_{min}(T) \|E\|^2 + 2 \quad \lambda_{max}(S) \|B_h\| \gamma_{max} \|E\|.$$

Consider the well-known inequality

$$ab \le z a^2 + \frac{b^2}{4z},$$

for any real parameters a, b, and $z > 0$.

Let $z = \theta \lambda_{min}(T)$ with $0 < \theta < 1$; then, the time-derivative of the Lyapunov function is bounded by

$$\dot{V}(E) \le -(1-\theta)\lambda_{min}(T)\|E\|^2 + \frac{\lambda_{max}(S)^2 \gamma_{max}^2 \|B_h\|^2}{\theta \lambda_{min}(T)}$$

Thus, the solution of this inequality is given by

$$V(t) \le \left(V(0) - \frac{\vartheta}{\nu} \right) e^{-\nu t} + \frac{\vartheta}{\nu},$$

where $\nu = (1-\theta) \frac{\lambda_{min}(T)}{\lambda_{max}(\mathrm{S})}$; $\vartheta = \frac{\lambda_{max}(S)^2 \gamma_{max}^2 B_h^2}{\theta \lambda_{min}(T)}$.

It follows that $E(t)$ is uniformly bounded for all $t \ge 0$ and the dynamic error converges to the compact set

$$S = \left\{ E \,|\, \|E\| \le \sqrt{\frac{\vartheta}{\lambda_{\min}(S)\nu}} \right\}.$$

We can conclude that the steady-state error is proportional to the amplitude of both noises and uncertainties that affect the flight dynamics. In the matched case (without noises and uncertainties), the closed system is asymptotically stable and the tracking error, given in equation (12) or (13), converges to the origin.

C. POSTION CONTROL

To control the position of the aircraft in the (x-y) plan, the cascade structure is used. The rotational dynamics, included in sub-system1 (4a), are very high compared to the dynamics of sub-system 2 (4b). Therefore, the rotational dynamics (sub-system: $\prod_1$) described in (4b) is considered as the inner loop while the translational dynamics (sub-system: $\prod_2$) as the external loop.

Let us consider the position of the aircraft given by $Z_3 = |x \ y|^T$ and the desired position is given by $Z_{3ref} = |x_{ref} \ y_{ref}|^T$. Assuming small changes in pitch angle ($\cos(\phi) \approx 1$), the dynamic of the flight position becomes

$$\Pi_2 \begin{cases} \dot{Z}_3 = Z_2 \\ \dot{Z}_2 = \dfrac{F}{M} \Upsilon(\psi) V_i(t) \end{cases} \quad (15)$$

where $\Upsilon(\psi) = \begin{vmatrix} \cos(\psi) & \sin(\psi) \\ \sin(\psi) & -\cos(\psi) \end{vmatrix}$; $V_i(t) = \begin{vmatrix} \sin(\theta) \\ \sin(\phi) \end{vmatrix}$. $V_i(t)$ is the input vector to the sub-system ($\prod_2$). Accordingly, for this external loop, the objective function is

$$J_p(t, V_i) = \frac{1}{2} e_p(t+h)^T Q_p e_p(t+h) + \frac{1}{2} V_i^T R_p V_i, \quad (16)$$

where $Q_p \in \mathcal{R}^{2\times 2}$ and $R_p \in \mathcal{R}^{2\times 2}$ are positive-definite matrices, and $e_p(t) = Z_3(t) - Z_{3ref}$ is the position tracking error. The control vector that minimizes the cost function (16) is given by

$$V_i(t) = -\frac{h^2}{2} \frac{T}{M} \left(\frac{h^4}{4} \frac{T^2}{M^2} \Upsilon(\psi)^T Q_p \Upsilon(\psi) + R_p \right)^{-1} \times \Upsilon(\psi)^T Q_p \left(e_p + h\dot{e}_p - \ddot{Z}_{3ref} \right). \quad (17)$$

We have to note that the reference signals θ_{ref} and ϕ_{ref}, used in equation (11), are given by

$$\begin{vmatrix} \theta_{ref} \\ \phi_{ref} \end{vmatrix} = \arcsin(V_i(t)).$$

This is the cascaded control structure, which is typically prescribed for systems involving time-scale separation assumption. That is, the rotational loop is designed to have a faster dynamic than the translational loop. Consequently, the desired targets of the translational movements $\xi_{ref} = \left| x_{ref} \ y_{ref} \ z_{ref} \right|^T$, chosen in continuous time, consist of step functions smoothed by means of second-order filters and are given as

$$\frac{\xi_{refi}}{\nu_{refi}} = \frac{\omega_i^2}{s^2 + 2\zeta_i\omega_i s + \omega_i^2},$$

where the index $i\,(i = 1, 2, 3)$ stands for x, y and z. The control parameters ζ_i and ω_i specify the dynamics of these filters in order to consider the time-scale separation between two loops.

Using the stability analysis, seen previously, we can state that the nonlinear system under the cascade structure closed by the control law (8) for both altitude and altitude control and (17) for position control is stable and the dynamic of the position error $e_p\,(t)$ and $E\,(t)$ are uniformly bounded.

D. INTEGRAL ACTION

Even though the tracking error of the proposed control approach is uniformly bounded, the steady state error, due to the payload variations and low-frequency disturbances, can be eliminated by including integral action in the altitude loop. To this end, the objective function of the altitude control, decoupled from sub-system (4a), is reformulated as follows

$$J_z = \frac{1}{2}q_z e_{z0}\,(t+h)^2 + \frac{1}{2}r_z F\,(t)\,, \tag{18}$$

where q_z and r_z are positive constants, $e_z\,(t) = z\,(t) - z_{ref}$, and $e_{z0}\,(t) = \int e_z\,(\tau)\,d\tau$. In this case, the deduced control signal is

$$F\,(t) = -\frac{6h^3 q_z \cos(\phi)\cos(\theta)\,M}{q_z h^6 \cos(\phi)^2\cos(\theta)^2 + 36M^2 r_z} \times \left(e_{z0}\,(t) + he_z\,(t) + \frac{h^2}{2}\dot{e}_z(t) + \frac{h^3}{6}\left(-g - \ddot{y}_{ref}\right)\right). \tag{19}$$

Note that, taking $r_z \approx 0$ and substituting it in the altitude dynamic equation, we obtain the dynamic of the altitude position with the integral action as

$$\frac{h^3}{6}\dddot{e}_{z0} + \frac{h^2}{2}\ddot{e}_{z0} + h\dot{e}_{z0} + e_{z0} = 0, \tag{20}$$

which is asymptotically stable for any $h > 0$.

IV. SIMULATION RESULTS

To check the effectiveness of the proposed control algorithm, computer simulations are conducted using MATLAB/SIMULINK software. The solver used in the simulation utilizes a fixed step size with a sample time $T_s = 0.01\ s$ (sample frequency of *100 Hz*). The numerical values of the parameters of the UAV used in [1] are given as follows

$$\begin{aligned} I &= 10^{-3} diag\left(7.5\ 7.5\ 13.3\right) kg.m^2; \\ M &= 0.65 kg; \\ \alpha &= 3.1310^{-5} Ns^2;\ \beta = 7.510^{-7} Nms^2; \\ J_r &= 610^{-5} kg.m^2;\ l = 0.23m; \\ \epsilon &= 0.01m, \quad \varepsilon = 0m,\ g = \frac{9.81m}{s^2}. \end{aligned}$$

To maintain the cascade structure and ensure the stability of the overall system a suitable selection of control parameters is required. Therefore, after some tuning, adequate control parameters are chosen as:

- For the attitude: $h = 0.1$; $Q = 10^2 I_3$; $R = 10^{-2} I_2$.
- For the altitude: $h = 0.5$; $q_z = 10^2$; $r_z = 10^{-2}$; $\zeta = 1$; $\omega_z = 0.5 rad/s$.
- For the position control: $h = 1$; $Q_p = 10^2 I_2$; $R_p = 10^{-2} I_2$; $\zeta = 1$; $\omega_p = 2 rad/s$.

During the simulation, all initial positions of the flight are set to zero, i.e. $x\,(0) = y\,(0) = z\,(0) = 0m$; $\theta\,(0) = \phi\,(0) = \psi\,(0) = 0 rad$.

Simulations are first performed to check the performances of the closed-loop system with the controller given in (8), i.e. without the integral action. In order to check the effect of the payload variation on the flight, in the matched case, external disturbances and gusty winds are not considered. It is desired to lift an unknown payload of *6 N* at $t\ =0s$ and to deliver it to the position $Z_{ref} = 4m$ at $t = 8$s.

Figure 2 shows the altitude of the aircraft and its desired trajectory with the payload variation. The effect of the payload variation on the height position is evident. As expected, this unknown payload induced a steady-state error; thus, the payload is delivered in the wrong position. Note that for $t > 8$s, the load vanished and the height position converged to the desired trajectory.

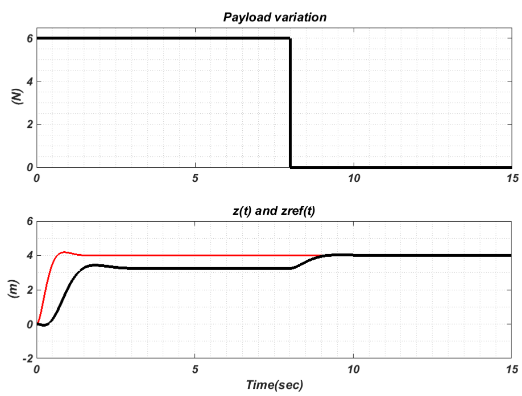

FIGURE 2. Altitude and its reference trajectory with the payload variation.

Second, simulations are carried out to check the robustness of the proposed algorithm in the mismatched case. Note that this mismatched case has not been considered in the work presented in [36]. In this case, it is desired to move the aircraft from its initial position (origin) to the desired position $\left|-1\ -1\ 4\right|^T$.Then, it hovers for a while at the position $\left|0\ 0\ 4\right|^T$ to drop off the payload at $t = 20s$ and it returns back to the position $\left|0\ 0\ 0.5\right|^T$.

In addition to the load variation, the mismatched case is considered as follows:

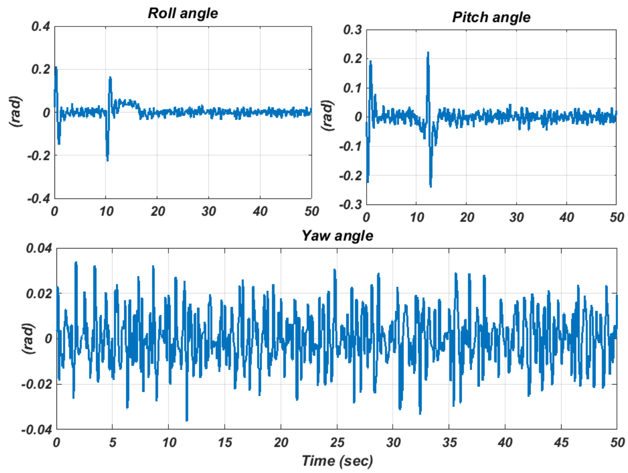

FIGURE 3. Attitude variations of the craft during the flight.

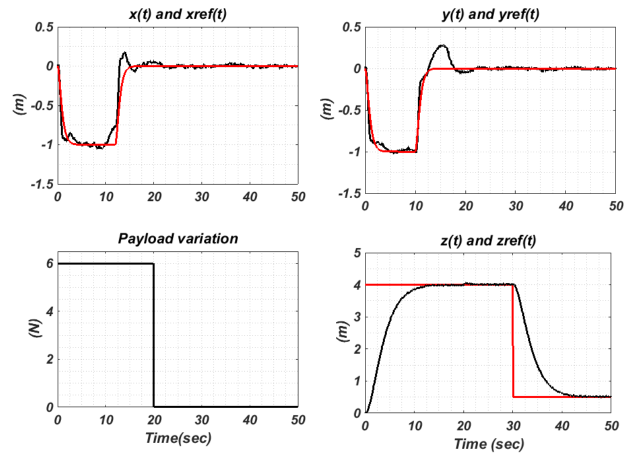

FIGURE 4. Altitude, position and its reference trajectories with payload variation.

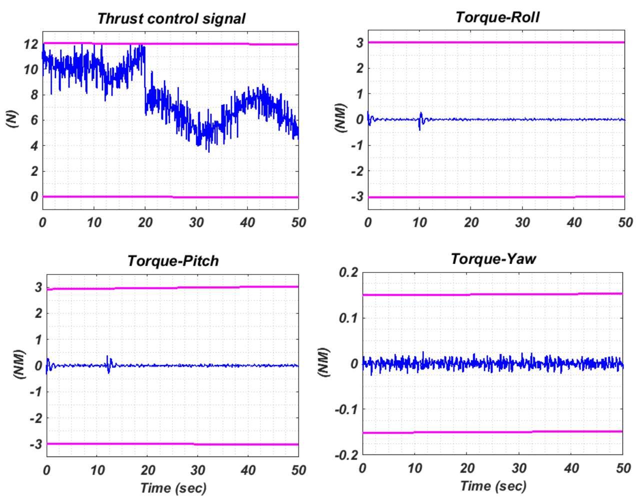

FIGURE 5. Applied control signals: thrust and torques.

1) The external disturbances acting on translational and the rotational dynamics are modeled as [32]

$$F_x(t) = 0.5(\nu(t) - \nu(t-4)) + 0.01 \sin\left(\frac{\pi t}{10}\right),$$
$$F_y(t) = 0.5(\nu(t) - \nu(t-4)) + 0.1 \sin(4\pi t),$$
$$F_z(t) = 0.1 sin(4\pi t) + 2\cos\left(\frac{\pi t}{10}\right), \quad (21)$$

where $\nu(t)$ is the unit step signal.

2) Constraints on control signals: As it is stated in the introduction, the advantage of the proposed controller in comparison with other nonlinear controllers is in its ability to include explicitly the constraints of the control signals in the control design. In this case, the goal of the one-step-ahead predictive control method with integral action is to minimize the following constrained cost function:

$$J(t, y, U) = \frac{1}{2}\|\bar{e}(t+h)\|^2_{\bar{Q}} + \frac{1}{2}\|U(t)\|^2_R, \quad (22)$$

subject to the constraints $U_{min} \leq U(t) \leq U_{max}$, where $\overline{Q} \in \mathcal{R}^{5\times 5}$ is a positive definite matrix, $\bar{e}(t) = |e_{z0} \quad e|^T = |e_{z0} \quad e_z \quad e_\phi \quad e_\theta \quad e\psi|^T$; $U(t) = \begin{vmatrix} U_1 & U_2 & U_3 & U_4 \end{vmatrix}^T$.

The constraints on the control vector $U(t)$ are explicitly related to the speed of the four rotors that can be expressed as

$$0 \leq U_1 \leq 4\alpha\omega^2_{max},$$
$$-\alpha\omega^2_{max} \leq U_{2,3} \leq \alpha\omega^2_{max},$$
$$-2\beta\omega^2_{max} \leq U_4 \leq 2\beta\omega^2_{max}.$$

Using the fact that the maximum thrust force of the quadcopter is $F_{max} = 4\alpha\omega^2_{max} \geq \max(Mg + L(t)) = 12.376\,N$, the constraints on the control vector are then given as $U_{min} = \begin{vmatrix} 0 & -3 & -3 & -0.15 \end{vmatrix}^T$ and $U_{max} = \begin{vmatrix} 12 & 3 & 3 & 0.15 \end{vmatrix}^T$.

The solution of the quadratic optimization problem (22) is applied to the aircraft under the payload variation, disturbances (21) and normally distributed noise measurements ($\sigma^2 = 0.01$). In [36] the constraints on the speed of four motors were not considered. Therefore, in [36] the controller is given in closed form.

Figure 3 depicts the behavior of the roll, pitch, and yaw of the craft during the flight, which are close to the desired references.

The simulation results in figure 4 show that good tracking performances are achieved. The results below demonstrate that the nonlinear predictive algorithm with integral action has strong robustness properties in the presence of load disturbances, wind gusts, and noise measurements. Hence, from these results, one can conclude that the proposed one-step-ahead predictive controller can achieve robust altitude stabilization during the VTOL of an unmanned aerial vehicle in the presence of external disturbances and payload variation.

Figure 5 depicts the deduced control signals from the optimization of the constrained objective function (22) in the mismatched case. We notice that all control signals are within the saturation limits. Figure 6 shows the scenario when the unknown load has been increased to $8N$ and the thrust control is constrained to $U_{1max} = 11.8N$. The quadrotor, closed by the proposed algorithm, was able to track the desired

TABLE 2. Comparison of the proposed algorithm with several recent methods.

Advantages	Control methods				
	PID [1]	SMC [37]	Back stepping[38]	FNMPC [39]	OSAMPC
Constraints handling	No	No	No	Yes	Yes
Robustness with respect to payload variations.	Not tested	Not tested	Not tested	Not tested	Yes
Providing the stability proof.	No	Yes	Yes	No	Yes
Robustness with respect to noises and wind gusts.	No	Yes	Yes	Yes	Yes
Easy to code (the control loop is given in closed form).	Yes	Yes	Yes	No	Yes

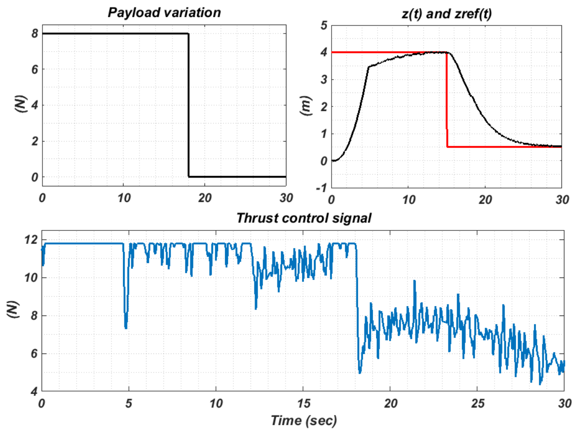

FIGURE 6. Altitude and the applied thrust control signal.

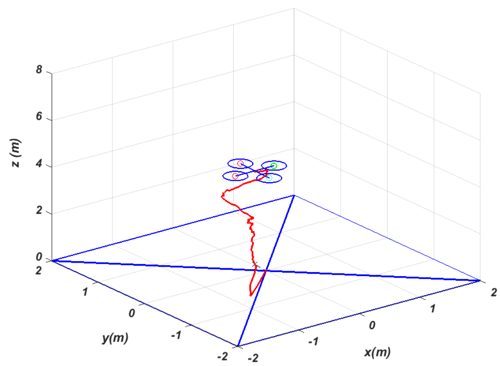

FIGURE 7. Altitude and attitude of the UAV during the hovering mission.

reference trajectory despite the fact that the payload was unknown and variable. Further, the deduced thrust magnitude lies inside the saturation limits. Table II lists different achievements of some robust nonlinear controllers; it is clear that each control method has its own limitation. Indeed, for the case where the effect of the payload variation is not tested (especially in [1], [37], [38]), these algorithms may eliminate the steady-state error since they incorporate integral action in the loop. However, the induced control signals that lie outside the saturation limits will produce poor tracking performances, and even the instability as stated in [29].

The solution is to use the control approach that includes the constraints in the controller design. Therefore, we can conclude that the proposed control algorithm (OSAMPC) integrates all benefits of the recent robust nonlinear control approaches.

Figure 7 illustrates the position, altitude, and attitude of the UAV at time $t = 15\ s$, during its hovering mission before dropping off the payload. Note that Corke [35] developed the 3D plot function used in this simulation.

V. CONCLUSION

This study presented a simple nonlinear control algorithm to solve the problem of delivering a payload by a quadcopter to the desired height in the presence of uncertainties, noise measurements, and wind gusts. A quadrotor model is a complex nonlinear system with six DOF and four inputs (underactuated system).

Various nonlinear control methods have been proposed in the literature to solve the payload transportation problem in a complex environment; however, each method has its own limitation. In this paper, we show that using a cascade structure control design, based on the one-step-ahead nonlinear predictive controller with integral action, is effective to solve the mentioned control problem.

The designed controller ensures the boundedness of all tracking errors. In fact, it was demonstrated, by means of the Lyapunov method, that the tracking errors are uniformly bounded. Further, constraints on control signals have been included in the control design, where a quadratic optimization problem is solved to deduce the optimal solution. Simulations, which were carried out using a real model of a quadrotor, illustrate the accurate position stabilization of altitude and attitude in the presence of uncertainties, noises and wind disturbances with faster payload disturbance rejection. Therefore, the algorithm is robust, computationally inexpensive, and suitable for onboard real-time implementation.

In this work, full-state measurement was assumed and used for the control design. Therefore, additional research should be oriented first towards the construction of an observer to estimate the state, and second towards the discrete time implementation of the continuous-time one-step-ahead predictive controller on a real platform.

ACKNOWLEDGMENT

The authors are grateful for the support from the Research Center of the College of Computer and Information Sciences, King Saud University.

REFERENCES

[1] S. Bouabdallah, "Design and control of quadrotors with application to autonomous flying," Ph.D. dissertation, École Polytechnique Fédérale Lausanne, Lausanne, Switzerland, 2007.

[2] A. Mokhtari, A. Benallegue, and B. Daachi, "Robust feedback linearization and GH$_\infty$ controller for a quadrotor unmanned aerial vehicle," in *Proc. IEEE/RSJ Int. Conf. Intell. Robots Syst. (IROS)*, Edmonton, AB, Canada, Aug. 2005, pp. 1198–1203.

[3] L. Malconi, A. Isidori, and A. Serrani, "Autonomous vertical landing on an oscillating platform: An internal-model based approach," *Automatica*, vol. 38, no. 4, pp. 21–32, 2002.

[4] J. M. Pflimlin, P. Sourès, and T. Hamel, "Position control of a ducted fan VTOL UAV in crosswind," *Int. J. Control*, vol. 80, no. 5, pp. 666–683, 2007.

[5] N. Guenard, T. Hamel, and V. Moreau, "Dynamic modeling and intuitive control strategy for an 'X4-flyer,'" in *Proc. Int. Conf. Control Automat. (ICCA)*, Budapest, Hungary, Jun. 2005, pp. 142–146.

[6] T. Madani and A. Benallegue, "Control of a quadrotor mini-helicopter via full state backstepping technique," in *Proc. IEEE 45th Conf. Decis. Control*, San Diego, CA, USA, Dec. 2006, pp. 1515–1520.

[7] R. Xu and U. Ozguner, "Sliding mode control of a quadrotor helicopter," in *Proc. 45th IEEE Conf. Decis. Control*, San Diego, CA, USA, Dec. 2006, pp. 4957–4962.

[8] O. Shakernia, Y. Ma, T. Koo, and S. Sastry, "Landing an unmanned air vehicle: Vision based motion estimation and nonlinear control," *Asian J. Control*, vol. 1, no. 3, pp. 128–145, 1999.

[9] M. A. M. Basri, A. R. Husain, and K. A. Danapalasingam, "Intelligent adaptive backstepping control for MIMO uncertain non-linear quadrotor helicopter systems," *Trans. Inst. Meas. Control*, vol. 37, no. 3, pp. 345–361, 2015.

[10] G. Antonelli, E. Cataldi, F. Arrichiello, P. R. Giordano, S. Chiaverini, and A. Franchi, "Adaptive trajectory tracking for quadrotor MAVs in presence of parameter uncertainties and external disturbances," *IEEE Trans. Control Syst. Technol.*, vol. 26, no. 1, pp. 248–254, Jan. 2018.

[11] A. Roberts and A. Tayebi, "Adaptive position tracking of VTOL UAVs," *IEEE Trans. Robot.*, vol. 27, no. 1, pp. 129–142, Feb. 2011.

[12] H. Wang and M. Chen, "Trajectory tracking control for an indoor quadrotor UAV based on the disturbance observer," *Trans. Inst. Meas. Control*, vol. 38, no. 6, pp. 675–692, 2016.

[13] S. Omari, M.-D. Hua, G. Dugard, and T. Hamel, "Nonlinear control of VTOL UAVs incorporating flapping dynamics," in *Proc. IEEE/RSJ Int. Conf. Intell. Robots Syst. (IROS)*, Tokyo, Japan, Nov. 2013, pp. 2419–2425.

[14] T. Lee, "Robust adaptive attitude tracking on SO(3) with an application to a quadrotor UAV," *IEEE Trans. Control Syst. Technol.*, vol. 21, no. 5, pp. 1924–1930, 2013.

[15] L. Besnard, Y. B. Shtessel, and B. Landrum, "Control of a quadrotor vehicle using sliding mode disturbance observer," in *Proc. Amer. Control Conf.*, New York, NY, USA, Jul. 2007, pp. 5230–5235.

[16] T. Dierks and S. Jagannathan, "Output feedback control of a quadrotor UAV using neural networks," *IEEE Trans. Neural Netw.*, vol. 21, no. 1, pp. 50–66, Jan. 2010.

[17] H. J. Kim, D. H. Shim, and S. Sastry, "Nonlinear model predictive tracking control for rotorcraft-based unmanned aerial vehicles," in *Proc. Amer. Control Conf.*, Anchorage, AK, USA, May 2002, pp. 3576–3581.

[18] E. N. Hartley, J. L. Jerez, A. Suardi, J. M. Maciejowski, E. C. Kerrigan, and G. A. Constatinides, "Predictive control using an FPGA with application to aircraft control," *IEEE Trans. Control Syst. Technol.*, vol. 22, no. 3, pp. 1006–1017, May 2014.

[19] P. J. Gawthrop, H. Demircioglu, and I. Siller-Alcala, "Multivariable continuous-time generalised predictive control: A state-space approach to linear and nonlinear systems," *IEE Proc. Control Theory Appl.*, vol. 145, no. 3, pp. 241–250, 1998.

[20] P. Lu, "Optimal predictive control of continuous nonlinear systems," *Int. J. Control*, vol. 62, no. 3, pp. 633–649, 1995.

[21] R. Hedjar, R. Toumi, P. Boucher, and D. Dumur, "Cascaded nonlinear predictive control of induction motor," *Eur. J. Control*, vol. 10, no. 1, pp. 65–80, 2004.

[22] N. Michael, J. Fink, and V. Kumar, "Cooperative manipulation and transportation with aerial robots," *Auton. Robots*, vol. 30, no. 1, pp. 73–86, 2011.

[23] N. S. Zúñiga, F. Muñoz, M. A. Márquez, E. S. Espinoza, and L. R. G. Carrillo, "Load transportation using single and multiple quadrotor aerial vehicles with swing load attenuation," in *Proc. Int. Conf. Unmanned Aircr. Syst. (ICUAS)*, Dallas TX, USA, Jun. 2018, pp. 269–278.

[24] K. Sreenath, N. Michael, and V. Kumar, "Trajectory generation and control of a quadrotor with a cable-suspended load—A differentially-flat hybrid system," in *Proc. IEEE Int. Conf. Robot. Automat.*, Karlsruhe, Germany, May 2013, pp. 4888–4895.

[25] M. Gharibi, R. Boutaba, and S. L. Waslander, "Internet of drones," *IEEE Access*, vol. 4, pp. 1148–1162, 2016.

[26] R. D'Andrea, "Can drones deliver?" *IEEE Trans. Autom. Sci. Eng.*, vol. 11, no. 3, pp. 647–648, Jul. 2014.

[27] D. Schneider, "Air traffic control for delivery drones," *IEEE Spectr.*, vol. 54, no. 1, pp. 32–33, Jan. 2017.

[28] F. Kandoul, "Modélisation et commande de véhicules aériens autonomes, et développement d'un pilote automatique basé sur la vision," Ph.D. dissertation, Heudiasyc Lab., Univ. Technol. Compiègne, Compiègne, France, 2007.

[29] G. C. Goodwin, S. F. Graebe, and M. E. Salgado, *Control System Design*. Upper Saddle River, NJ, USA: Prentice-Hall, 2000.

[30] J. P. How, C. Fraser, K. C. Kulling, L. F. Bertuccelli, O. Toupet, L. Brunet, A. Bachrach, and N. Roy, "Increasing autonomy of UAVs: Decentralized CSAT mission management algorithm," *IEEE Robot. Autom. Mag.*, vol. 16, no. 2, pp. 43–51, Jun. 2009.

[31] Z. Xue, J. Wang, Q. Shi, G. Ding, and Q. Wu, "Time-frequency scheduling and power optimization for reliable multiple UAV communications," *IEEE Access*, vol. 6, pp. 3992–4005, 2018.

[32] L. Wang and J. Su, "Trajectory tracking of vertical take-off and landing unmanned aerial vehicles based on disturbance rejection control," *IEEE/CAA J. Automatica Sinica*, vol. 2, no. 1, pp. 65–73, Jan. 2015.

[33] J. Hauser, S. Sastry, and G. Mayer, "Nonlinear control design for slightly non-minimum phase systems: Application to V/STOL aircraft," *Automatica*, vol. 28, no. 4, pp. 665–679, 1992.

[34] A. Isidori, I. Marconi, and A. Serrani A. "Robust autonomous guidance: An internal model approach," in *Advances in Industrial Control*. New York, NY, USA: Springer Verlag, 2003.

[35] P. Corke, *Robotics, Vision and Control: Fundamental Algorithms in MATLAB*, 2nd ed. Berlin, Germany: Springer-Verlag, 2017.

[36] R. Hedjar, "Robust one-step-ahead model predictive control of VTOL-UAVs," in *Proc. 227th Chin. Control Decis. Conf. (CCDC)*, Qingdao, China, May 2015, pp. 23–25.

[37] I. Gonzalez-Hernandez, S. Salazar, R. Lopez, and R. Lozano, "Altitude control improvement for a quadrotor UAV using integral action in a sliding-mode controller," in *Proc. Int. Conf. Unmanned Aircr. Syst. (ICUAS)*, Arlington, VA, USA, Jun. 2016, pp. 711–716.

[38] S. Bouabdallah and R. Siegwart, "Full control of a quadrotor," in *Proc. IEEE/RSJ Int. Conf. Intell. Robots Syst.*, San Diego, CA, USA, Oct./Nov. 2007, pp. 153–158.

[39] M. Kamel, K. Alexis, M. Achtelik, and R. Siegwart, "Fast nonlinear model predictive control for multicopter attitude tracking on SO(3)," in *Proc. IEEE Conf. Control Appl. (CCA)*, Sydney, NSW, Australia, Sep. 2015, pp. 1160–1166.

[40] S. Li, Y. Wang, J. Tan, and Y. Zheng, "Adaptive RBFNNs/integral sliding mode control for a quadrotor aircraft," *Neurocomputing*, vol. 216, pp. 126–134, Dec. 2016.

[41] R. A. Barrón-Gómez, L. E. Ramos-Velasco, E. S. E. Quesada, and L. R. G. Carrillo, "Wavelet neural network PID controller for a UAS transporting a cable-suspended load," *IFAC-PapersOnLine*, vol. 50, no. 1, pp. 2335–2340, Jul. 2017.

[42] E. Kayacan and R. Maslim, "Type-2 fuzzy logic trajectory tracking control of quadrotor VTOL aircraft with elliptic membership functions," *IEEE/ASME Trans. Mechatronics*, vol. 22, no. 1, pp. 339–347, Feb. 2017.

[43] Y. Wang and S. Boyd, "Fast model predictive control using online optimization," *IEEE Trans. Control Syst. Technol.*, vol. 18, no. 2, pp. 267–278, Mar. 2010.

[44] X. Zhao, X. Wang, S. Zhang, and G. Zong, "Adaptive neural backstepping control design for a class of nonsmooth nonlinear systems," *IEEE Trans. Syst., Man, Cybern. Syst.*, to be published.

[45] X. Huo, L. Ma, X. Zhao, and G. Zong, "Observer-based fuzzy adaptive stabilization of uncertain switched stochastic nonlinear systems with input quantization," *J. Franklin Inst.*, vol. 356, no. 4, pp. 1789–1809, 2019.

[46] H. Wang, P. X. Liu, X. Xie, X. Liu, T. Hayat, and F. E. Alsaadi, "Adaptive fuzzy asymptotical tracking control of nonlinear systems with unmodeled dynamics and quantized actuator," *Inf. Sci.*, to be published. doi: 10.1016/j.ins.2018.04.011.

RAMDANE HEDJAR (M'09–SM'16) received the Ph.D. degree in electronic and electrical engineering from USTHB University, Algeria, in collaboration with SUPELEC (Paris-France), in 2002.

After finishing his Ph.D. degree, he joined the Computer Engineering Department, King Saud University, as an Assistant professor. From 1992 to 2000, he was a Lecturer with the Department of Electronics, Djelfa University. From 1994 to 2000, he was a Research Assistant with the Electronic Department, BLIDA University. He is currently a Professor with the Department of Computer Engineering, King Saud University. His research interests include robust control, nonlinear predictive control, robotics, neural network control, and networked control systems.

MANSOUR ABDULAZIZ AL ZUAIR received the B.S. degree in computer engineering from King Saud University, Riyadh, Saudi Arabia, and the M.S. and Ph.D. degrees in computer engineering from Syracuse University, Syracuse, NY, USA.

He served as the Chairman of the Computer Engineering Department, King Saud University (2003–2006), the Vice Dean (2009–2015), and has been the Dean of the College of Computer and Information Sciences, since 2016. He is currently an Associate Professor with the Department of Computer Engineering, College of Computer and Information Sciences, King Saud University. His research interests include computer architecture, computer networks, and signal processing.